Sridharan Ravi[a], Caroline Ponraj[b]

[a] Department of Physics, Mepco Schlenk Engineering College, Sivakasi, India
[b] Department of Physics, VIT, Chennai, India

Synthesis and characterization of new Bi_2FeNiO_6 material using a citric acid assisted gel combustion technique

Multiferroic materials, which show simultaneous ferroelectric and magnetic ordering, exhibit unusual physical properties – and in turn promise new device applications – as a result of the coupling between their dual order parameters. $BiFeO_3$ is currently considered the most promising candidate material for device applications of room temperature multiferroics. However, its G-type antiferromagnetic behavior and high Néel temperature restrict the use of this material in potential applications. We report the synthesis and characterization of a novel Bi_2FeNiO_6 material for the first time using a citric acid assisted gel combustion technique. Magnetization studies reveal that it exhibits ferrimagnetism with Néel temperature around 500 K. Differential scanning calorimetry study also reveals a sharp phase transition at 500 K. These materials also exhibit good ferroelectric behavior with square type hysteresis with a remanent polarization (P_r) of 1.28 μC cm^{-2}, saturation polarization (P_s) of 18 μC cm^{-2} and coercive fields 20 kV and -40 kV respectively. The results are convincing to make a big step towards developing devices that run on spin.

Keywords: Multiferroics; Spintronics; BFO; Ferromagnetic order; Gel combustion

1. Introduction

Multiferroics belong to the family of multifunctional oxides in which ferroelectric, ferromagnetic, and ferroelastic behaviors coexist in the same materials system. Today the definition has been extended to include other long-range orders like anti ferromagnets as well. However, it has become a trend to use the term "multiferroics" to mean the materials which have both spontaneous magnetic and electrical ordering simultaneously. If there is a coupling between their order parameters, these materials exhibit an interesting physical phenomenon called the magnetoelectric (ME) effect [1]. Recent years have witnessed a great interest in magnetoelectric multiferroics in which ferroelectric and magnetic orders not only coexist in the same material, but also couple with each other such that the magnetic degree of freedom can be manipulated by an electric field and vice versa.

Multiferroics materials are very rare and in fact we have only a very few material in nature. Hill [2] studied the reasons for the same. It has also been found that both ferromagnetic and ferroelectric ordering are mutually exclusive, leading to a scarcity of magnetic ferroelectrics due to the so-called "d^0 vs d^n problem". That is, while the ferroelectric materials have transition metal ions with empty d shells (e. g., Ti^{4+} ions in $BaTiO_3$), ferro-, ferri- and antiferro- magnetic materials require the presence of (3d) transition metals or ions with partially filled d shells. Against this well-known scarcity of the magnetic ferroelectrics, in an ABO_3 perovskite oxide, the stereo-chemically active $6s^2$ lone pair electrons of Bi^{3+} (and Pb^{2+}) ions in the A-site offers an alternative way to get the ferroelectric ordering irrespective of the kind of (magnetic) ions present in the B-site. Khomskii reported an excellent review article which mainly suggests tools to combine magnetism and ferroelectricity [3]. The multiferroic materials $BiFeO_3$, $BiMnO_3$, $BiCrO_3$ and Bi_2FeCrO_6 are some of them which fall in this category [4, 5].

Among these, $BiFeO_3$ has been quite extensively studied due to its high antiferromagnetic and ferroelectric ordering temperatures, $T_N = 643$ K and $T_C = 1\,123$ K respectively. But, it's G-type antiferromagnetic structure is modulated to a spiral spin structure, whose modulation vector has a long period of $\lambda_q = 620$ Å [6–16]. This spiral spin structure averages out the net magnetic moment over the length λ_q to zero and the induced magnetization varies linearly with the applied magnetic field without any remanent magnetization. It also inhibits the possibility of measuring appreciably high linear ME effect. But, substitution of aliovalent (heterovalent) ions to the Bi^{3+} ions was found to destroy this incommensurately modulated spin structure and favors the homogeneous spin structure that establishes spontaneous magnetization in $BiFeO_3$ [17]. The above mentioned observations and the possibility of getting ferroelectric order by charge ordering [18, 19] motivated us to synthesize a novel $BiFeO_3$ (BFO) based multiferroic material. The first report on BFO was given by Smolenskii [19] followed by many workers. Kim et al. [20] report the simple synthesis procedure of BFO powder via a sol-gel route. But bulk powders have very high magnetic ordering and hence exhibit multiferroicity at low temperatures. This was subsequently reported by Das et al. [21]. They reported ferroelectric properties of BFO thin film grown by sputtering. But this report failed to show ferroelectric coupling and the magnetoelectric nature of BFO. Vijayanand et al. [22] synthesized $BiFeO_3$ nanopowder via an autocombustion method where

210

Int. J. Mater. Res. (formerly Z. Metallkd.) 104 (2013) 2

the fuel used was glycine. They studied the magnetic properties of the nanoparticles above and below room temperature. They also found that the synthesized particles had an impurity phase of magnetite which contributed to the high ferromagnetic moment of the material. Ryu et al. [23] successfully reported the magnetic nature of BFO grown on strontium titanate (STO) substrates, but ferromagnetic ordering was found to be very weak. Yan et al. [24] reported enhanced multiferroic ordering at room temperature of BFO by doping with Ru. But ferroelectric ordering was weak and Ru is too costly to use for commercial applications. Uniyal and Yadav [25] have studied the multiferroic property of Eu doped BFO. According to their study the Eu doped BFO has found to exhibit a weak ferromagnetism and a saturated polarization at room temperature. This uneven ordering of this material disqualifies it for any device applications. Kim et al. [26] studied the Co and Ta substituted in $BiFeO_3$ ceramics but these materials hardly possess good electrical tunability. Shimakawa et al. [27] synthesized a new multiferroic compounds with double-perovskite structures. High-pressure synthesis was employed in synthesizing Bi_2NiMnO_6 in bulk form and also in a thin film form by epitaxial growth. However, it was found that the material exhibited the multiferroic property only at low temperature, making it unsuitable for device application. Singh et al. [28] synthesized and studied the multiferroic property of $(Bi_{0.9}Pb_{0.1})(Fe_{0.9}Ti_{0.1})O_3$. From their results, the synthesized material exhibit room temperature multiferrocity. But the synthesized material is found to have some traces of impurities. The main disadvantage is using lead, which is not eco-friendly making it an unsuitable candidate for further applications. Interesting results were given by Gheorghiu et al. [29], but low temperature range restricts to use it in real time applications.

From the above review it is clear that we are in need of good multiferroic material that possesses equal coexistence of ferroelectric and ferromagnetic material. Feng [30] has given an ab-initio prediction of the coexistence of the ferrimagnetism and ferroelectricity in rhombohedral Bi_2FeNiO_6 (hereafter referred as BFNO). According to their prediction this novel material exhibits a ferrimagnetism of 1.86 μ_B and polarization of 23.05 $\mu C\, cm^{-2}$. In this paper, we have tried to make this theoretical work reality by developing a new Bi_2FeNiO_6 nanomaterial and have shown that it possesses good ferroelectric and ferromagnetic behavior that can be used for potential applications.

2. Material and methods

One of the most widely used and useful method of preparation of BFO is the combustion synthesis route using a fuel. The fuel may be either L-α-alanine and glycine [31] or urea [32]. We have used citric acid as fuel in our present work. Bismuth iron nickel oxide was prepared via the gel combustion method using citric acid as the fuel. 0.01 mol of iron nitrate, 0.01 mol of bismuth nitrate and 0.01 mol of nickel nitrate were used as precursors. Initially, bismuth nitrate was dissolved in nitric acid because it is insoluble in water. Then, to the solution, 0.01 mol of iron nitrate, 0.01 mol of nickel nitrate and 0.04 mol of citric acid was added. 100 ml of water was added to the resulting mixtures and mixed in a beaker. The *pH* of the solution was found to be 2. To convert the metal nitrates to the corresponding oxides

the pH was raised to nine by adding ammonia solution. The mixture was then heated and evaporated on a hot plate with stirring till it became a dark viscous resin. Continuous heating leads to the auto-ignition of the dried resin with the evolution of large quantities of gases. The ashes from the self ignition of the resin were calcined in a furnace for one hour at 600 °C, to obtain the required material.

The crystal structure and phase composition of the powders were determined using an X-ray diffractometer (XRD) using X'pert PRO, PANalytical diffractometer with nickel-filtered Cu-K_α radiation under ambient and scanning in the 2θ range of $10–90°$, in steps of $0.016°$. The particle size and morphology were observed using field emission scanning electron microscopy (SEM) (HITACHI SUI510 scanning electron microscope operating at 1 kV equipped with an energy dispersive X-ray (EDX) analysis unit. The shape and features of the multiferroic BFNO nanoparticles was analyzed using a Park system XE70 atomic force microscope. Differential scanning calorimetry (DSC) (DSC 204 F1, NETZSCH, Germany) of BFNO powders was carried out using the model Mettler Toledo DSC 822e with a resolution of 0.04 mW at RT. The magnetic properties of the BFNO powders were measured using a vibrating sample magnetometer (VSM) at room temperature. A TF anlayser 2000 and PE loop tracer were used to study the electric polarization behavior of the sample.

3. Results and discussion

Figure 1 shows the XRD patterns of the gel combustion synthesized BFNO powders calcined at 600 °C for one hour. It was found that the BFNO nanoparticles exhibited the crystalline nature of a rhombohedral distorted perovskite structure. All the reflections in the experimental patterns are somewhat broad indicating the nanocrystalline nature of the sample. The average crystallite size is calculated to be 35 nm from the Scherrer formula. It is also found that the intensity profiles of the reflection peaks are close to that of the reported JCPDS (# 86-1518 and # 031169) for bismuth ferrite and (BiNi) [33]. XRD also shows the phase purity of our sample and no other phases or impurities exist. Figure 2 illustrates an SEM image of the pure BFNO, which was crystallized at 600 °C in N_2 atmosphere followed by leaching in nitric acid. The BFNO powders show soft agglomerates of irregular-shaped particles of 100 nm in size. This demonstrates that the gel combustion process is a good method for preparing nanoscale BFNO particles with uni-
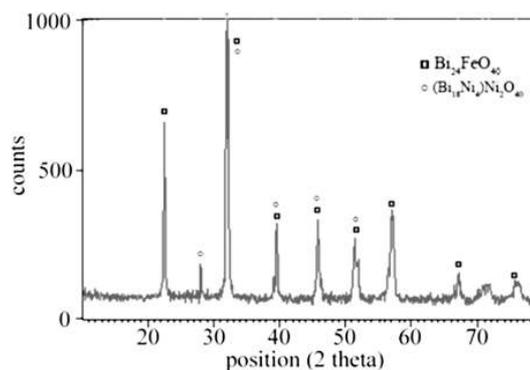

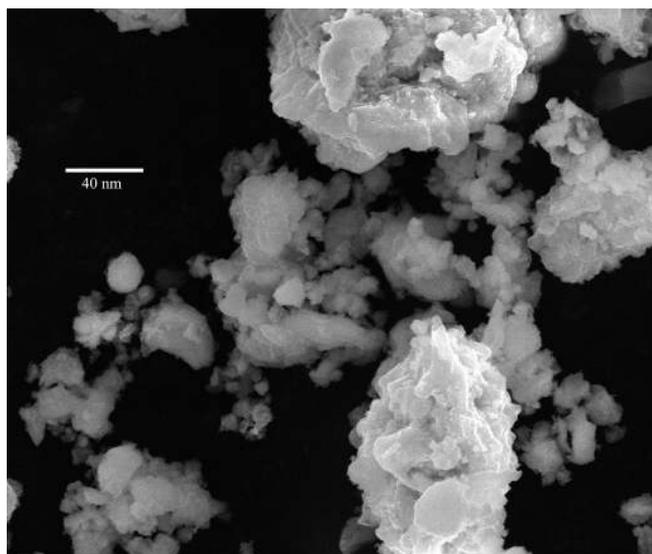Fig. 1. XRD pattern of Bi_2FeNiO_6 powder calcined at 600 °C for 1 h showing the presence of bismuth nickel ferrite in nanophase.

Fig. 2. SEM image of BFNO powder calcined at 600 °C for 1 h showing soft agglomerates of irregular-shaped particles.

form features. From the EDS measurement in Fig. 3, it is confirmed that the atomic ratios of Bi/Fe/Ni are in good proportion forming nanocrystalline BFNO. From the EDX profile it is clear that there are no impurities present. The peaks excluding the bismuth, iron, nickel and oxygen peaks shown in the EDS spectra originate from the substrate used for SEM observation. The table in Fig. 3 gives the elemental composition of the sample along with their weight and atomic percentages. From the table it is clear that the atomic ratio of Fe : Ni is almost one. But the presence of bismuth in the compound is very much low compared to iron and nickel. This is because bismuth oxide is volatile and so there will be a loss of bismuth oxide during sintering. This problem would have been easily overcome by using an excess amount of bismuth nitrate in the synthesis process compared to iron and nickel nitrate. Figure 4 shows the 3-D AFM image of the BFNO nanoparticles. The particles

also exhibited a homogeneous distribution and the particle size was found to be around 20 nm. The AFM image was taken in a non-contact mode and the scanning area is 10 μm in the x-axis and 10 μm in the y-axis. Line profile analysis of the image is also presented in Fig. 4. A line is drawn along the x-axis at around 6 μm and it is found that the maximum height of the particle along the line is in the range of 12 nm and another line was drawn along the y-axis at 4.5 μm and the maximum width along this line is found to be 5 nm.

The thermal behavior of the sample was studied using the DSC. Figure 5 shows the DSC pattern of BFNO nanoparticles. The DSC curve was obtained over a temperature range from 30 K to 600 K at the rate of 10 K min^{-1}. From the observed data it is clear that two important endothermic reactions take place at 542 K. A sharp peak at 542 K may be attributed to magnetic ordering (T_N) temperature of BFNO and it seems it is much lower than previously reported values [34–37]. A high transition temperature or so-called Néel temperature restricts the potential use of materials for spintronics devices [38]. From the DSC study, it is reasonable to presume that a strong phase transformation has occurred at 542 K (possibly from ferrimagnetic to paramagnetic). However, this can be confirmed only by detailed magnetic study. The other peak at the higher end may be due to the presence of small impurities of iron oxide which undergo a phase transformation at that temperature.

The M–H hysteresis loop is presented in Fig. 6, where a and b show the hysteresis behavior of BFNO samples at 100 K, 200 K. At 100 K and 200 K the sample exhibits coercive fields of 386.4 G and 379.75 G and a remanent magnetization of 0.29185 emu and 0.28568 emu. At room temperature the material exhibits a coercive field of 384.82 G and retentivity of 0.28515 emu (presented in Fig. 6). From these data it is clear that BFNO exhibit hysteresis behavior at 100 K, 200 K and 300 K with not much change in either saturation magnetization or retentivity. This seems to be interesting however; the reasons for this behavior are not understandable. Figure 7 shows the M–H curve at 400 K and 300 K and it clearly shows a drastic dif-

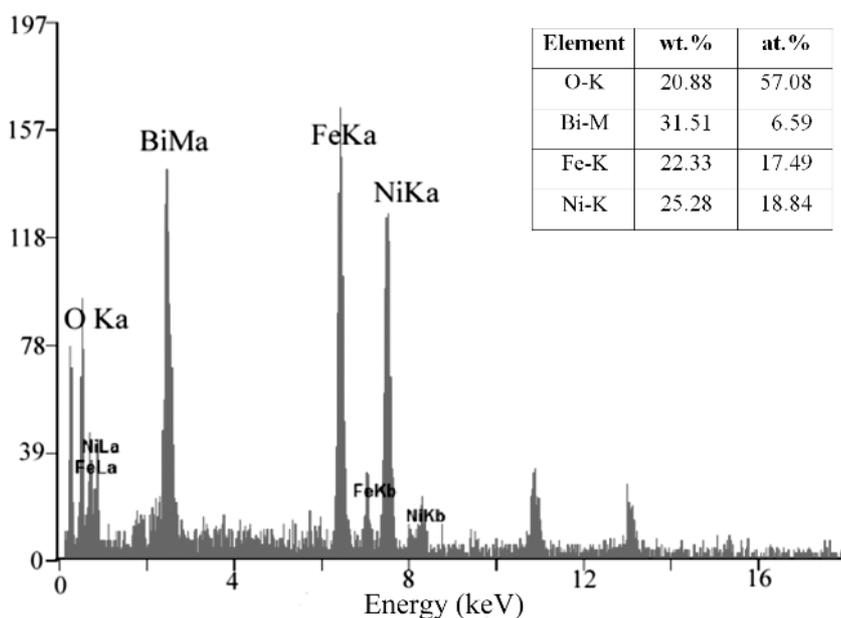| Element	wt. %	at. %
O-K	20.88	57.08
Bi-M	31.51	6.59
Fe-K	22.33	17.49
Ni-K	25.28	18.84

Fig. 3. EDX profile with elemental composition of BFNO showing no impurties in the synthesized nanopowder.
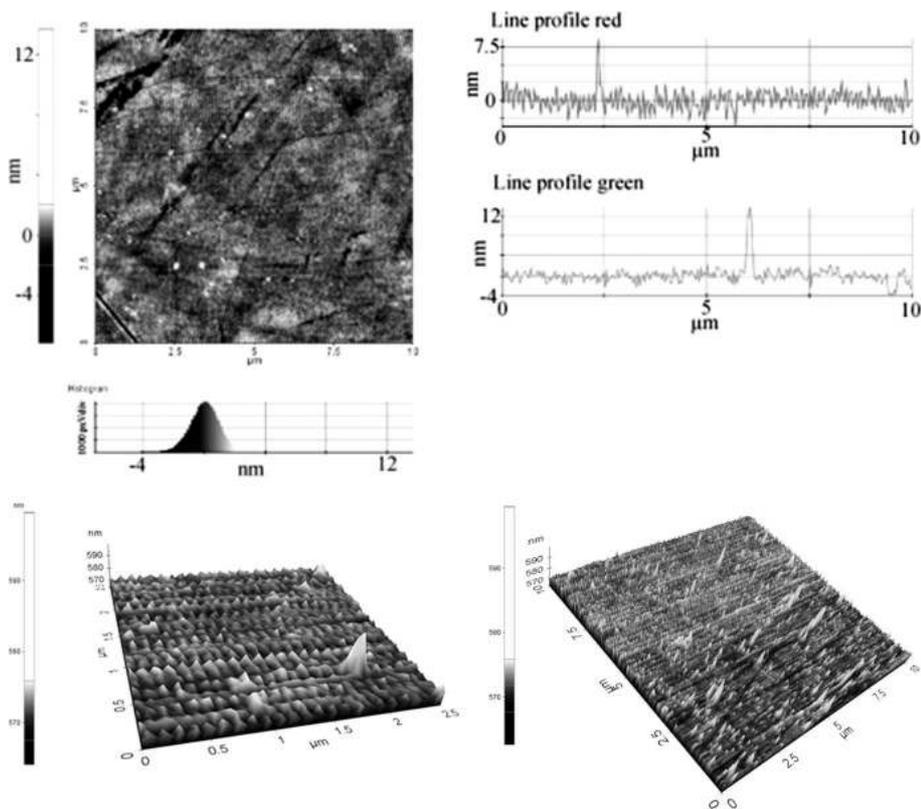
Fig. 4. AFM images of the BFNO powder showing homogenous distribution of particle size around 20 nm Top: Line profile image. Bottom: Cropped 3D-image.

ference in the hysteresis behavior at 400 K. In order to illustrate the magnetic ordering in BFNO, the temperature dependence of zero-field-cooled (ZFC) and field-cooled (FC) magnetization curves are presented in Fig. 8. In these measurements, the sample was cooled in either ZFC to a desired temperature and then a magnetic field was applied or FC. The measurements were made while warming the sample in the magnetic field for both cases. A field of 1 000 G was applied for the ZFC and FC measurements. The ZFC and FC plot clearly describes that the curie temperature of the sample is well above room temperature, thereby overcoming one of the main problems faced by the existing multiferroics. From the graph it is found that the blocking temperature is around 214 K and cluster spin glass (magnetic disorder exchange interaction between antiferromagnetic and ferromagnetic) is observed at low temperature below 73 K. ZFC and FC diverges at 525 K. For ZFC the magneti-

zation increases slowly by decreasing the temperature and reaches maximum at 214 K and started to decrease. For FC, the magnetization increases with decrease in temperature and small change is observed near 300 K and 100 K. Beyond 525 K ZFC and FC converges and no change is observed up to 600 K. To predict the Néel temperature, we can fix the divergence point (525 K) as the transition temperature or need to study the magnetization behavior at higher temperature. The temperature vs magnetization was studied and is presented in the Fig. 9. The magnetization was almost steady up to 500 K and shows a sharp decrease at 500 K. From this it is clear that Néel temperature was in 500 K as confirmed by DSC results. From these observations, it could be concluded that the sample BFNO is not G-type antiferromagnetic material and may be ferrimagnetic as predicted ab-initio [28] with a Néel temperature close to 500 K. The results obtained from DSC and ZFC-FC/high temperature magnetization are reasonably in the range of 500 K. The almost constant magnetization may be due to strong Fe–Ni interaction and this interaction also results in residual magnetization. Since the Néel temperature is close to room temperature this would be more suitable for potential applications.

The presence of ferroelectricity in BFNO is indicated by the ferroelectric hysteresis loop measured at room temperature as shown in Fig. 10. Square type hysteresis behavior is observed with a remanent polarization (P_r) of 1.28 μC cm^{-2}, spontaneous polarization (P_s) of 18 μC cm^{-2} and coercive fields 20 kV and –40 kV respectively. The values agree well with the theoretical results [30] and are higher than for the $BiFeO_6$ sample and most particularly the square type behavior assists good electrical switching characteristics for device applications.
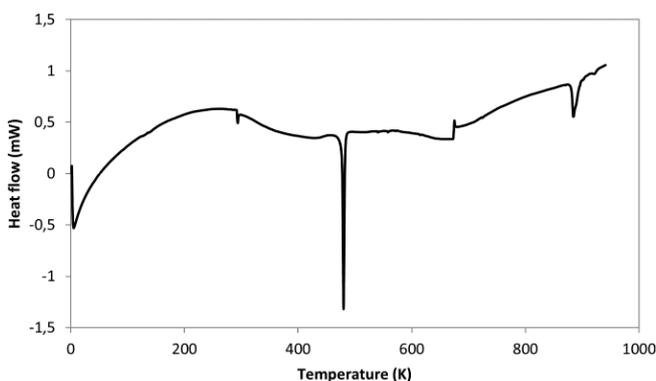

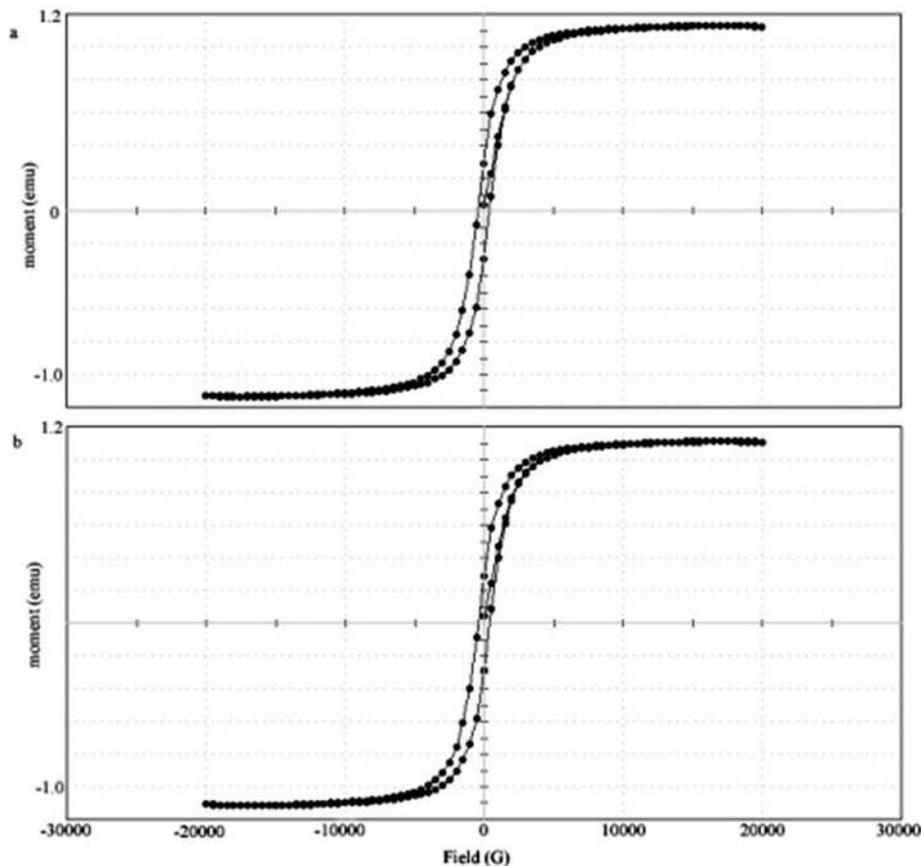Fig. 5. DSC curve of BFNO nanopowder showing a sharp peak at 542 K.

Fig. 6. *M–H* curve of BFNO at low temperature (where $a = 100$ K, $b = 200$ K) showing almost same type of hysteresis at 100 K and 200 K.
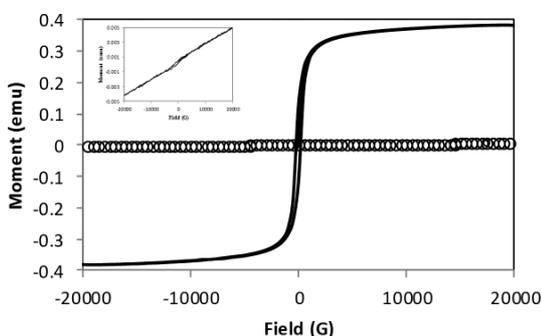

Fig. 7. *M–H* curve of BFNO at room temperature and at 400 K (red line is for 400 K and black hysteresis is for 300 K) showing drastic difference in hysteresis behavior at 400 K. Inset shows the magnified view at 400 K.
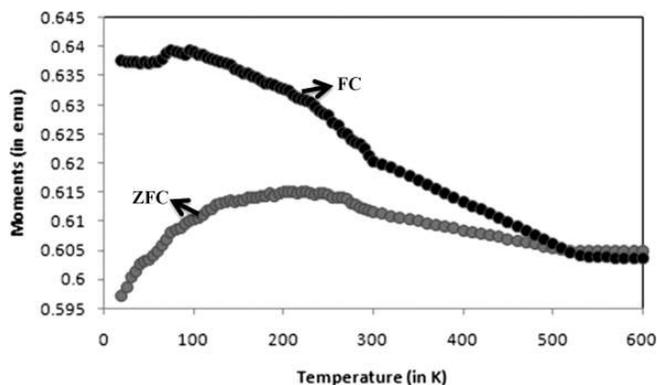

Fig. 8. ZFC-FC measurements of BFNO nanopowder showing convergence at 525 K (Red circles is for ZFC and brown circles for FC).
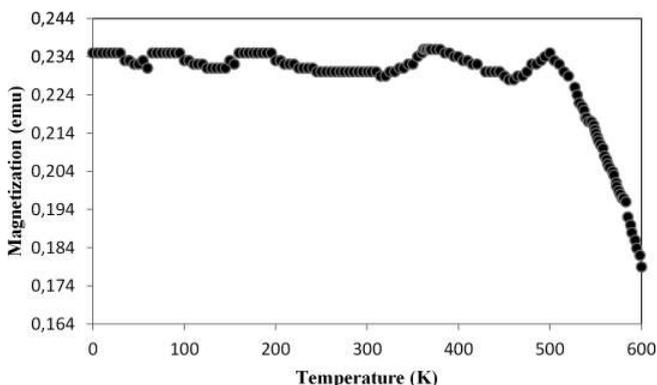

Fig. 9. High temperature magnetization study on BFNO nanopowder showing almost constant magnetization up to 500 K.
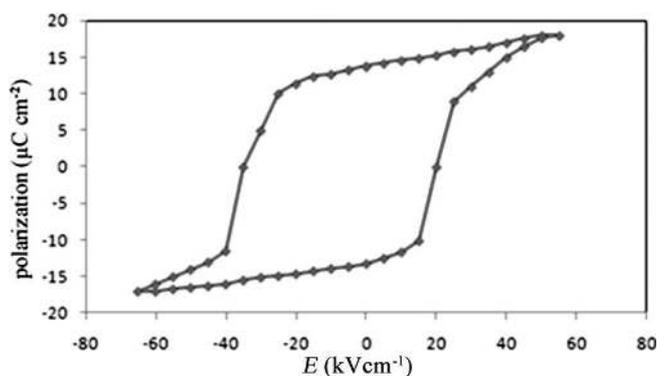

Fig. 10. *P–E* curve of BFNO nanopowder showing square type hysteresis.

4. Conclusion

In conclusion, Bi_2FeNiO_6 nanoparticles were synthesized successfully using the gel combustion technique and characterized using XRD, SEM and AFM. From the results obtained from the multiferroic study, we can conclude that all the above mentioned materials exhibit a room temperature coexistence of ferrimagnetic and ferroelectric behavior. BFNO nanoparticles are found to exhibit enhanced ferromagnetism compared to others, with a coercive field of 384.85 G. This work can further be enhanced by using a different approach to synthesize nanoparticles and also by growing the BFNO film on different substrates. These materials are of great interest because of their magneto-electric multiferroic property at room temperature opening up new potential applications.

References

[1] R. Ramamoorthy, L. Martin: Multiferroics: Synthesis, characterization and applications, John Wiley & Sons, Limited (2012).
[2] N.A. Hill: Phys. Chem. B 104 (2000) 6694. DOI:10.1021/jp000114x
[3] D.I. Khomskii: J. Magn. Magn. Mater 306 (2006) 1. DOI:10.1016/j.jmmm.2006.01.238
[4] P. Baettig, C. Ederer, N.A. Spaldin: Phys. Rev. B 72 (2005) 8. DOI:10.1103/PhysRevB.72.214105
[5] T. Atou, H. Chiba, K. Ohoyama, Y. Yamaguchi, Y. Syono: J. Solid State Chem. 145 (1999) 639. DOI:10.1006/jssc.1999.8267
[6] P. Royen, K. Swars: Angew. Chem. 69 (1957) 779. DOI:10.1002/ange.19570692407
[7] G.A. Smolenskii, V.M. Yudin, E. Sher, Y.E. Stolypin: Sov. Phys.-JETP 16 (1963) 622
[8] D. Lebeugle, D. Colson, A. Forget, M. Viret: Appl. Phys. Lett. 91 (2007) 022907. DOI:10.1063/1.2753390
[9] S.V. Kiselev, R.P. Ozerov, G.D. Zhdanov: Sov. Phys.-Dokl. 7 (1963) 742.
[10] V.G. Bhide, M.S. Multani: Solid State Commun. 3 (1965) 271. DOI:10.1016/0038-1098(65)90031-1
[11] I. Sosnowska, T. Peterlin-Neumaier, E. Steichele: J. Phys. C: Solid State Phys. 15 (1982) 4835. DOI:10.1088/0022-3719/15/23/020
[12] F.P. Yu, A.K. Zvezdin, G.P. Vorob'ev, A.M. Kadomtseva, V.A. Murashev, D.N. Rakov: JETP Lett. 57 (1993) 69.
[13] D. Lebeugle, D. Colson, A. Forget, M. Viret, A.M. Bataille, A. Gukasov: Phys. Rev. Lett. 100 (2008) 227602. DOI:10.1103/PhysRevLett.100.227602
[14] H. Béa et al.: Appl. Phys. Lett. 87 (2005) 072508. DOI:10.1063/1.2009808
[15] S.K. Singh, H. Ishiwara, K. Maruyama: Appl. Phys. Lett. 88 (2006) 262908. DOI:10.1063/1.2218819
[16] N. Wang, J. Cheng, A. Pyatakov, A.K. Zvezdin, J.F. Li, L.E. Cross, D. Viehland: Phys. Rev. B 72 (2005) 104434. DOI:10.1103/PhysRevB.72.104434
[17] D.V. Efremov, J. Van den Brink, D.I. Khomskii: Nat. Mater. 3 (2004) 853. PMid:15558036; DOI:10.1038/nmat1236
[18] C. Ederer, N.A. Spaldin: Current Opinion in Solid State and Materials Science 9 (2005) 128. DOI:10.1016/j.cossms.2006.03.001
[19] G.A. Smolenskii, I.E. Chupis: Usp. Fiz. Nauk 137 (1982) 415. DOI:10.3367/UFNr.0137.198207b.0415
[20] J.K. Kim, S.S. Kim, W.J. Kim: Material Letters 59 (2005) 4006. DOI:10.1016/j.matlet.2005.07.050
[21] R.R. Das et al.: Appl. Phys. Lett. 88 (2006) 242904. DOI:10.1063/1.2213347
[22] S. Vijayanand, H.S. Potdar, P.A. Joy: Appl. Phys. Lett. 94 (2009) 182507. DOI:10.1063/1.3132586
[23] S. Ryu, J. Kim, Y. Shin, B. Park, J.Y. Son, H.M. Jang: Chem. Mater. 21 (2009) 5050. DOI:10.1021/cm9014496
[24] F. Yan, M. Lai, L. Lu: Phys. Chem. C 114 (2010) 6994.
[25] P. Uniyal, K.L.Yadav: J. Appl. Phys. 105 (2009) 07D914.
[26] W.S. Kim, Y.K. Jun, K.H. Kim, S.-H. Hong: J. Magn. Magn. Mater. 321 (2009) 3262. DOI:10.1016/j.jmmm.2009.05.059
[27] Y. Shimakawa, M. Azuma, N. Ichikawa: Materials 4 (2011) 153. DOI:10.3390/ma4010153
[28] K. Singh, R.K. Kotnala, M. Singh: Appl. Phys. Lett. 93 (2008) 212902. DOI:10.1063/1.3030989
[29] F.P. Gheorghiu, A. Ianculescu, P. Postolache, N. Lupu, M. Dobromir, D. Luca, L. Mitoseriu: J. Alloys Compd. 506 (2010) 862. DOI:10.1016/j.jallcom.2010.07.098
[30] H. Feng: Physica B 405 (2010) 2470. DOI:10.1016/j.physb.2010.03.011
[31] J. Yang, X. Li, J. Zhou, Yu Tang, Y. Zhang, Y. Li: J. Alloys Compd. 509 (2011) 9271. DOI:10.1016/j.jallcom.2011.07.023
[32] C. Paraschiv, B. Jurca, A. Ianculescu, O. Carp: J. Therm. Anal. Calorim. 94 (2008) 411. DOI:10.1007/s10973-008-9145-5
[33] Powder Diffraction data, International Center for Diffraction Data, Card 4-0835.
[34] Y.N. Venevtsev, G. Zhdanov, S. Solov'ev: Sov. Phys. Crystallogr. 4 (1960) 538.
[35] G. Smolenskii, V. Isupov, A. Agranovskaya, N. Krainik: Sov. Phys. Solid State 2 (1961) 2651.
[36] B. Ruette, S. Zvyagin, A.P. Pyatakov, A. Bush, J.F. Li, V.I. Belotelov, A.K. Zvezdin, D. Viehland: Phys. Rev. B 69 (2004) 064114. DOI:10.1103/PhysRevB.69.064114
[37] K. Sen, K. Singh, A. Gautam, M. Singh: Nanotechnology and Nanoscience 1 (2010) 0976.
[38] W. Kleemann, P. Barisov: Physics and Biophysics I (2008) 203.

Correspondence address

Dr. S. Ravi
Department of Physics
Mepco Schlenk Engineering College
Sivakasi 626005,
India
Tel.: +91 4562235691
Fax: +91 4562235111
E-mail: sravi@mepcoeng.ac.in

You will find the article and additional material by entering the document number **MK110844** on our website at *www.ijmr.de*

Int. J. Mater. Res. (formerly Z. Metallkd.) 104 (2013) 2

215